Systematic Design of THz Leaky-Wave Antennas based on Homogenized Metasurfaces

Walter Fuscaldo, *Student Member, IEEE,* Silvia Tofani, *Student Member, IEEE,* Dimitrios C. Zografopoulos,
Paolo Baccarelli, *Member, IEEE,* Paolo Burghignoli, *Senior Member, IEEE,*
Romeo Beccherelli, *Member, IEEE,* and Alessandro Galli, *Member, IEEE.*

Abstract—In this work, a systematic design of Fabry-Perot cavity antennas based on leaky waves is proposed in the THz range. The use of different topologies for the synthesis of homogenized metasurfaces shows that a specific fishnet-like unit-cell is particularly suitable for the design of efficient THz radiating devices. Accurate full-wave simulations highlight advantages and disadvantages of the proposed geometries, thoroughly considering the bounds dictated by technological constraints and the homogenization limit as well. The radiative performance of different designs for achieving theoretical directivities ranging from 15 dB to 30 dB is evaluated with reliable analytical and numerical methods, and completely validated with full-wave simulations. The relevant results corroborate the proposed systematic design, consolidating the validity and the usefulness of the leaky-wave approach, well-established at microwave frequencies, to the more challenging and still unexplored THz range.

Index Terms—Leaky-wave antennas (LWAs), leaky waves, Fabry-Perot cavity antennas, terahertz, metasurfaces.

I. INTRODUCTION

IN recent years, the fruitful combination of microwave and optical techniques has considerably narrowed the so-called 'THz gap', a term reflecting the lack of efficient THz components [1]. In spite of this remarkable progress, the demand of efficient THz antennas is still high [2], [3]. Indeed, even though various solutions have been proposed [4]–[6], such as lens-coupled antennas [7]–[9] and integrated horn antennas [10]–[12] to name but a few, the price for their superior radiating performance is paid in terms of high fabrication costs and complexity [6].

To develop flat, low-profile, and also reconfigurable THz planar antennas, graphene has been considered, exploiting the propagation of highly-confined surface plasmon polaritons (SPP) [13] in order to enhance radiation [14]–[16]. Despite the attractive reconfigurable properties and low-profile features of such graphene THz antennas, it has been shown that plasmonic losses dramatically affect the efficiency of these devices [17].

Graphene antennas based on nonplasmonic solutions have been proposed demonstrating that the efficiency can be recovered at the price of a reduced reconfigurability [18], [19]. In any case, the quality of graphene (which mainly determines its price and its reproducibility as well [20]) plays a key-role in determining the performance of such antennas. In this regard, recent works [21], [22] have also established the fundamental limitations in the performance of any graphene-based device.

Significant efforts are thus still needed to improve the performance of THz radiating systems. To this purpose, we propose here a systematic design of a specific class of THz antennas, namely Fabry-Perot cavity leaky-wave antennas (FPC-LWAs) [23], which allows for high radiating performance at a low cost and with low complexity of fabrication. To date, FPC-LWAs have been employed from microwave to the visible range, but in the THz range actual valid configurations are still lacking, except for graphene-based designs [18], [19].

Specifically, object of this study are those FPC-LWAs constituted by a grounded dielectric slab covered by a metallic patterned metasurface which acts as a partially reflecting sheet (PRS) [23]. Such periodic PRSs are studied in the homogenization limit [24] (i.e., with the period much smaller than the wavelength), so that a single impedance boundary condition suffices to accurately describe the electromagnetic response of the PRS as a whole. More precisely, an in-depth study of the effects of the geometry of the *unit-cell* on the value of the homogenized impedance is carried out for both *cermet*-and *fishnet*-like topologies [25], showing that some designs are more convenient than others to realize highly-reflective impedances, and thus improve the directivity of the FPC-LWA [26].

As a result of this analysis, a fishnet-like unit-cell is chosen to synthesize four different PRSs, which allow for achieving theoretical directivies of 15 dB, 20 dB, 25 dB, and 30 dB. The radiating performance of the four proposed designs is rigorously evaluated using both the leaky-wave approach and the reciprocity theorem (which accounts also for the contribution of the spatial wave [27]), and is then validated with full-wave results, showing a remarkable agreement. We should mention here that the proposed fishnet-like PRS has the following interesting features with respect to other existing PRSs: *(i)* it provides a very low purely imaginary impedance (and consequently a very high directivity) in the THz range without requiring extreme variation of its geometrical parameters when compared with similar homogenized metasurfaces such as patches or strips [28]; *(ii)* the high filling factor (the ratio between the

area covered by the metal and the unit-cell area) and the topologically-connected geometry make it particularly attractive in view of its potential use in a FPC-LWA filled with a tunable material (e.g., a liquid crystal [29]–[31]); by applying a driving voltage between the ground plane and the PRS it would then be possible to change the electromagnetic properties of the filling material, thus enabling beam-steering capabilities at fixed frequency as in graphene THz LWAs (see, e.g., [16], [17]). We also note that, differently from patches and strips for which there exist well-known homogenization formulas [28], no analytical formulas have been reported so far for such fishnet-like PRSs, thus motivating the in-depth study carried out in this work.

The paper is organized as follows: in Section II, the basic properties of FPC-LWAs are briefly reviewed. Section III is devoted to the impedance synthesis of different unit-cell topologies. In Section IV, the results of the previous Section are used to design four different FPC-LWA layouts whose radiating performance is then validated by numerical results and full-wave simulations. Finally, conclusions are drawn.

II. Fabry-Perot Cavity THz Leaky-Wave Antennas

The literature on FPC-LWAs is vast and their experimental realizations in the microwave range are numerous [23]. Here, we briefly summarize the main properties of this class of radiators, as they have already been extensively described in [23], [26].

From a general viewpoint, an FPC-LWA is a kind of 2-D quasi-uniform LWA (according to the classification provided in [23]) obtained as a *perturbation* of a metallic parallel-plate waveguide, where the upper plate is replaced with a PRS to permit radiation. Two specific features distinguish an FPC-LWA from other 2-D LWAs: *(i)* the thickness h of the slab is close to half a wavelength in the medium, $h \simeq 0.5\lambda_0/\sqrt{\varepsilon_r}$ (λ_0 and ε_r being the design wavelength in vacuum and the relative permittivity of the dielectric filling, respectively), to enhance a resonance condition which maximizes directivity at broadside [32]; *(ii)* as for most of quasi-uniform 2-D LWAs, the PRS is described by a single homogenized impedance [24].

The PRS can take various forms, e.g., a denser dielectric superstrate [32], a dielectric multilayer [33], or graphene [18]. Here, we focus only on those PRSs characterized by a periodic lattice of 'subresonant' elements, i.e., with period $p \ll \lambda_0$. Note that throughout the paper we assume to deal with a patterned metallic screen, treating the metal as a perfect electric conductor (PEC). Results are almost the same for thick enough good metals such as Cu, Ag, Al, Au, as discussed in Section IV.

The hypothesis $p \ll \lambda_0$ is also known as the *homogenization limit* [24], [28] and, as long as it is fulfilled (see Section IV for further assumptions), it allows for describing homogenized PRS by means of a purely imaginary impedance $Z_s = jX_s$ (no ohmic losses are expected for PRS made by PEC). Under these assumptions, FPC-LWAs are conveniently studied with an equivalent circuit model. The knowledge of the PRS impedance is provided by simple and accurate formulas for well-known geometries [28], [34] (e.g., patches, strips, etc.); otherwise, the value of the impedance can be obtained from full-wave simulations.
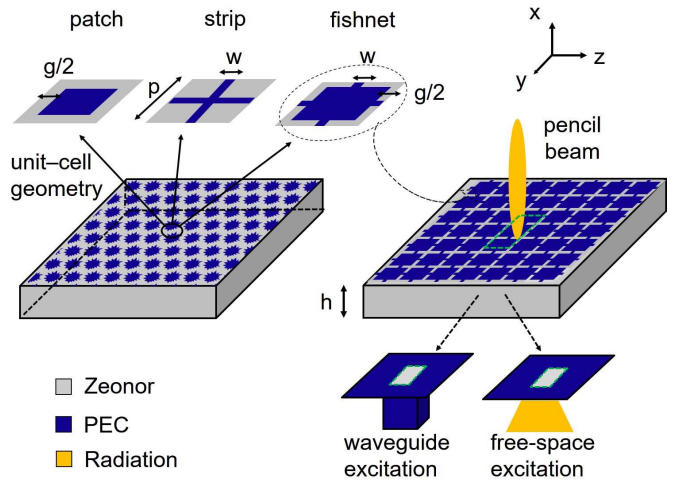

Fig. 1: Illustrative example of Fabry-Perot cavity leaky-wave antennas based on homogenized metasurfaces. At the upper-left corner, three different unit-cells of the homogenized metasurface are reported, along with their relevant geometrical parameters. The fishnet-like unit-cell is selected to obtain a directive ('pencil') beam as we show in Sections III and IV. At the bottom-right corner, two different types of excitation are illustrated: a slot etched in the ground plane, either fed by a waveguide or back-illuminated by a non-directive THz source.

Once Z_s is known, the transverse resonance technique [23] can be applied to the equivalent circuit model to derive the relevant dispersion equations, whose zeros represent the wavenumbers of the eigenmodes of the structure in both the bound (viz., surface waves), and the radiative (viz., leaky waves) regimes. Under certain conditions [35], [36], the fundamental TE-TM pair of leaky modes is sufficient to describe radiation from such FPC-LWAs. In these cases, the relevant complex *leaky* wavenumbers $k_z = \beta_z - j\alpha_z$, [$\beta_z$ and α_z being the phase and attenuation (or *leakage*) constant, respectively], for TE and TM polarizations allows for determining the radiating properties (i.e., the pointing angle and the beamwidth, mainly determined by β_z and α_z, respectively [23]) of the structure on the H- and E-plane, respectively (i.e., the xy- and xz-plane, respectively, with reference to the structure of Fig. 1) [37]. Interestingly, as long as $X_s \ll \eta_0$ ($\eta_0 \simeq 120\pi$ being the vacuum impedance), it has been shown [26] that the directivity at broadside D_0 is inversely proportional to the square of X_s:

$$D_0 \simeq (\sqrt{\varepsilon_r}/\pi)^{-2}(X_s/\eta_0)^{-2}. \tag{1}$$

whereas the fractional bandwidth FBW (defined as the range of frequency, normalized to the operating frequency, for which the radiated power density at broadside has decreased by less than 3 dB) is directly proportional to the square of X_s:

$$\text{FBW} = (2\sqrt{\varepsilon_r}/\pi)(X_s/\eta_0)^2 + \tan\delta_e, \tag{2}$$

where $\tan\delta_e$ is the loss tangent of the dielectric filling (which is non-negligible in the THz range).

As is manifest in Eqs. (1) and (2), a tradeoff is established between FBW and D_0. Consequently, lower values of X_s lead to highly-directive FPC-LWA working in a narrow bandwidth, whereas higher values of X_s lead to moderately-directive FPC-LWA working in a considerable bandwidth. Furthermore, when FPC-LWAs are designed in the THz range, one has to consider
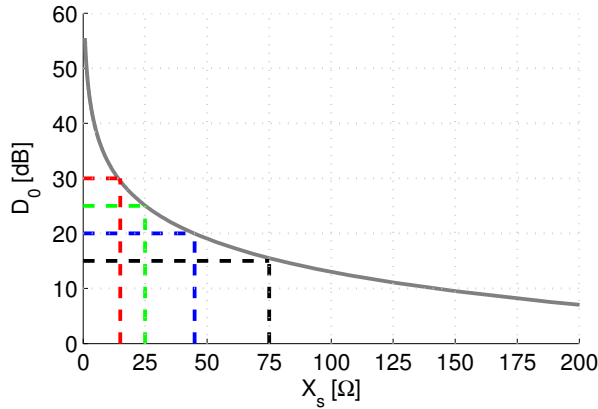
Fig. 2: Directivity at broadside D_0 vs. surface reactance X_s calculated as in Eq. (1). Black, blue, green, and red dashed lines higlight the values of the reactances required to achieve theoretical directivities of 15, 20, 25 and 30 dB, respectively.

several additional technological constraints: *(i)* the availability of low-loss THz materials, *(ii)* the availability of efficient THz sources, *(iii)* the fabrication tolerances. These practical considerations lead us to the following systematic design flow:

- With regard to *(i)*, a commercially available $h = 100~\mu m$ Zeonor substrate which exhibits among the lowest loss-tangents (viz., $\varepsilon_r = 2.3\,(1 - j0.001)$ [38]) in the THz range is considered. This fixes the design frequency to $f_0 = 1$ THz.

- With regard to *(ii)*, the FPC-LWA excitation will be obtained by etching a slot oriented along the y-axis in the ground plane; this can be either back-illuminated with a coherent THz source, or fed with a THz waveguide. The dimensions of the slot is set to 200 μm and 100 μm along the y- and z-axis (see Fig. 1), respectively, for a threefold reason. Firstly (considering guided-wave excitation), such dimensions are equal to the cross-section of commercial THz waveguides operating in the 900–1400 GHz band [39]. Secondly (considering free-space excitation), these dimensions provide a good energy coupling with commercial THz lenses (which focus the energy over a spot size of around 1 mm with a 2-D Gaussian profile [40]). Thirdly, these dimensions allow for modeling the slot as a (resonant-like) horizontal magnetic dipole (HMD) source, as required for exciting a pair of TE-TM leaky modes in a FPC-LWAs [23].

- With regard to *(iii)*, the unit-cell period of the PRS is set to $p = \lambda_0/5 = 60~\mu m$ to facilitate the PRS manufacturing (to fulfill the homogenization limit [28], p should preferably be smaller than $\lambda_0/4$. As a matter of fact, the smallest details commonly allowed in a standard photolithographic process should be greater than 3 μm to avoid fabrication issues in low-cost, large-area production [41]. The choice of $p = \lambda_0/5$ allows for designing details of the mask down to $p/20$.

On this basis, the next Section will focus on the synthesis of four suitable reactance values X_s to achieve theoretical directivities at broadside of 15, 20, 25, and 30 dB. Such values are theoretically realized with reactance values of 75, 45, 25,

and 15 Ω, respectively by means of Eq. (1), as is clear from Fig. 2, where D_0 has been calculated for $0 < X_s < 200~\Omega$. Obviously, as X_s increases, Eq. (1) looses accuracy (since it has been derived for $X_s \ll \eta_0$) and should be intended as an upper bound.

III. PROPERTIES OF HOMOGENIZED METASURFACES

We use HFSS to derive the reactance values X_s for different PRS geometries with $p = \lambda_0/5$ at $f_0 = 1$ THz. The unit-cell, constituted by the PRS etched at the interface between two different homogeneous dielectric media, is excited with a Floquet wave. The surface impedance is then retrieved from the simulated S-parameters [28]. The PRS consists of square patches, strips, and fishnet-like elements (see Fig. 1). The latter are obtained as a *superposition* of strips and patches. All elements are symmetric along the principal planes as discussed in Subsection III-C. The reactance X_s of the PRSs is evaluated for a wide variation of their relevant geometrical parameters, i.e., the gap g for the patches, the width w for the strips, and the combinations of both g and w for the fishnet. Specifically, g and w have been varied with step $0.05p$ from $0.05p$ to $0.4p$, which represent the lower and upper bounds dictated by fabrication tolerances (see Section II) and homogenization limit considerations [28], respectively.

The simulations have been initially carried out at a single frequency $f_0 = 1$ THz since it is expected that, as long as $X_s \ll \eta_0$, the operating frequency f_{op} does not differ significantly from the design frequency f_0. The results of the simulations are reported in Figs. 3(a)-(c) for all the considered geometries. As expected, the reactance of the patch-based PRS is negative (see Fig. 3(a)) due to its dominant capacitive behavior. As the gap decreases, the absolute value of the impedance decreases and the capacitive effect increases. Conversely, the reactance of strip-based and fishnet-based PRS is positive due to their dominant inductive behaviors (see Fig. 3(b)). It is worth noting here that the absolute value of X_s for a patch-based PRS is never lower than 100 Ω, thus revealing that a patch geometry is not suitable for the design of a directive THz FPC-LWA [see Eq. (1)]. Although it is possible to decrease the impedance value of patch-based PRSs by employing more complex geometries, e.g., a double-sheeted array [42] or Huygens' metasurfaces with anisotropic sheet impedance [43], such cases are not here considered as it goes beyond the scope of this work.

Conversely, the strip-based PRS can achieve values of X_s as low as 30 Ω for large widths (with respect to the period) of the strips. Moreover, reactance values greater than 30 Ω do not allow to achieve theoretical directivities greater than 25 dB. (The impact of substrate losses will be analyzed further.)

A. Impedance Synthesis of Fishnet Metasurfaces

As a possible solution, we have considered the fishnet-like element obtained as a superposition of patches and strips of the same dimensions. As shown in Fig. 3(c), this geometry has many advantages with respect to the previous configurations. As a matter of fact, the fishnet design allows for spanning values of X_s from 100 Ω to few ohms in the same parameter
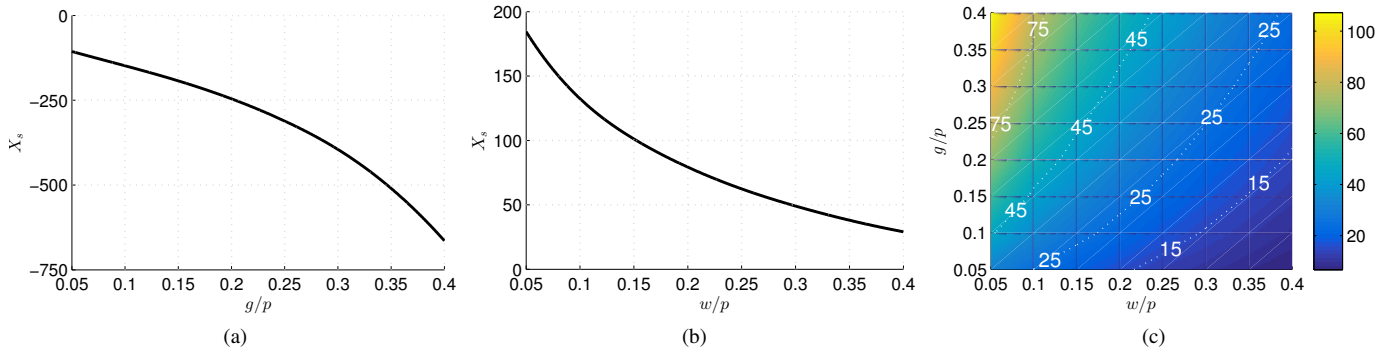
Fig. 3: Surface reactance X_s of (a) a patch-based PRS as a function of the gap g between the patches, (b) a strip-based PRS as a function of the width w of the strips, (c) a fishnet-based PRS as a function of both g and w. In (c) the iso-lines of the reactance at 15, 25, 45, and 75 [Ω] are reported in white dashed lines. All PRSs have a periodicity of $p = \lambda_0/5$.

space. Thus, highly directive FPC-LWAs can be designed using a suitable combination of g and w values. In fact, since the fishnet element has a two-valued space parameter, the designer has more degrees of freedom to synthesize the required values of the impedance: any pair of g and w lying on the iso-lines at 15, 25, 45 and 75 Ω [see white dotted lines in Fig. 3(c)] satisfies the corresponding impedance value. Note also that even a very low value of X_s such as 15 Ω can be synthesized without requiring an extreme parameter variation. Conversely, an extreme variation is needed for strip-based PRSs.

Furthermore, the filling factor FF of the fishnet is evidently larger than that of the single strip or patch equivalent design. This is an additional remarkable property of the fishnet element in the light of its use in a FPC-LWA filled with a tunable material such as a liquid crystal [29]–[31]. As recently demonstrated [30], the electric field applied across the fishnet plates permits almost a total reorientation of the optical axis of a liquid crystal; such a property is highly attractive for the development of THz reconfigurable antennas. Note that this would not be possible in a patch-based PRS (which has a comparable filling factor) due to the intrinsic *cermet* topology which does not allow for biasing the whole PRS with a single pair of electrodes.

B. Spatial Dispersion of Fishnet Metasurfaces

As shown in [24], [28], the grid impedance of patches for TE polarization and that of strips for TM polarization exhibit a spatially-dispersive character. Interestingly, we show here that the grid impedance of an array of fishnet-like unit-cells exhibits almost negligible spatial dispersion. In Fig. 4(a) the surface reactance X_s of a fishnet unit-cell of period $p = \lambda_0/10$, and geometrical parameters $g = w = p/10$, has been simulated in the frequency range $0.5 < f < 1.5$ THz, for angles of incidence varying from $\theta = 0°$ to $\theta = 80°$ referred to the vertical x-axis (colors gradually shade from blue to red).

The HFSS simulations confirm that the surface reactance of the fishnet-like unit-cell is essentially spatially nondispersive. Interestingly, we have verified with numerous HFSS simulations (not shown here for brevity) that this property is exhibited by all the unit-cells with fishnet-like topology, regardless of their geometrical parameters (provided that they are within the homogenization limit). We note that the spatially-nondispersive property of the fishnet-like elements might be of particular interest for future designs which take into account the possibility to dynamically steer the beam, as in [29].

C. Modal Coupling of Fishnet Metasurfaces

A low TE-TM modal coupling is fundamental to reasonably treat the surface impedance as a scalar value (as has always been considered in this work). Indeed, the homogenization approximation allows to write the surface impedance as a dyadic quantity $\underline{\mathbf{Z}}_s$ where the diagonal elements are related to the TE-TM polarizations, whereas the off-diagonal elements are related to the TE-TM cross-coupling [24]. Therefore, to first reduce $\underline{\mathbf{Z}}_s$ to a diagonal matrix, it should be verified that the TE-TM cross coupling of the fishnet-like unit-cell is negligible.

To this purpose, in Fig. 4(b) we have reported the values of the coupling between the TE and the TM polarizations in both reflection S_{11} and transmission S_{21} (due to reciprocity the S-matrix is symmetric) for incidence at $\phi = 45°$ (ϕ being the azimuthal angle measured from the y-axis to the z-axis, see Fig. 1) and $\theta = 0°, 40°, 80°$ on the same fishnet design of Fig. 4(a) (results were qualitatively the same for the fishnet layouts proposed throughout the paper). As can be seen, the amount of coupling is always negligible (below -70 dB) for any angle θ (we have reported only three values for clarity purposes), even in the case $\phi = 45°$ where the maximum TE-TM cross-coupling is expected (the coupling being absent for plane-wave incidence along the symmetry planes of the structure, i.e., for $\phi = 0°$ and $\phi = 90°$). This property allows us to consider $\underline{\mathbf{Z}}_s$ as a diagonal matrix. Moreover, since we are interested in the behavior of $\underline{\mathbf{Z}}_s$ at normal incidence $\theta = 0°$, there is no distinction between the diagonal elements, and thus $\underline{\mathbf{Z}}_s$ can safely be treated as a scalar value. Even more, the spatially-nondispersive character of the fishnet element, together with the symmetry of the structure along the principal planes allows us to use such a scalar value even for $\theta \neq 0°$; this consolidates the validity of the dispersion analysis shown in the next Section IV.

To summarize, the proposed fishnet element looks the preferred choice for the modeling of the PRS since it allows a flexible synthesis of the surface impedance. These elements
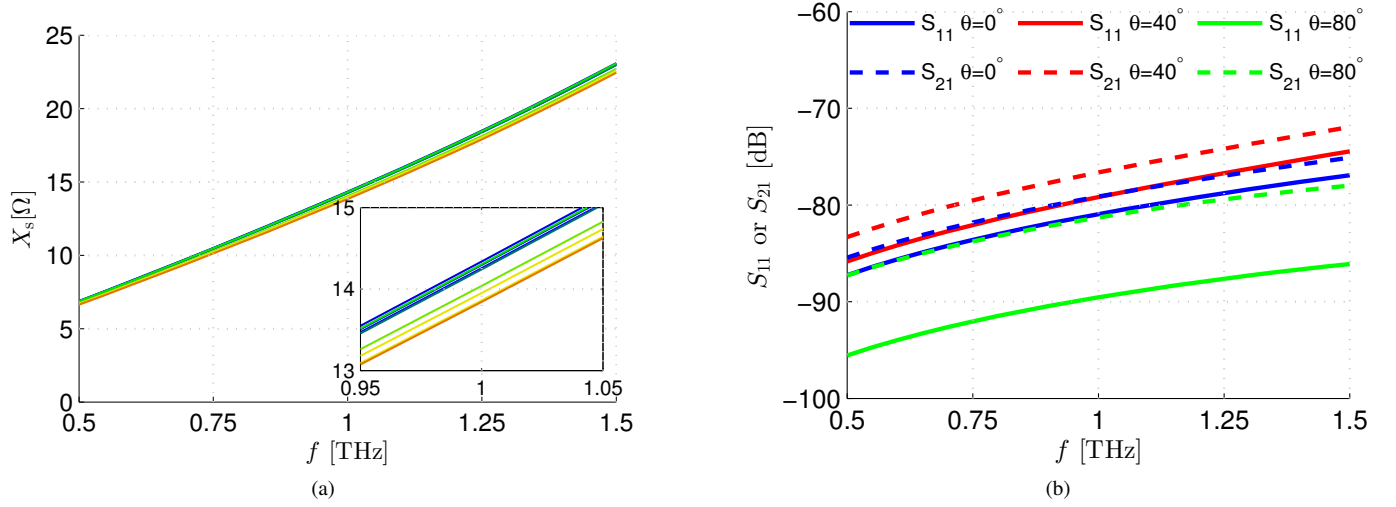
Fig. 4: (a) Surface reactance X_s vs. frequency f of a fishnet-like unit-cell (parameters in the text) for the angle of incidence θ ranging from $0°$ (blue) to $80°$ (red) with an angular step of $10°$ (as shown in the inset the color shades from blue to red as θ increases). As is seen, the curves are all enveloped in a tight bundle (see the inset), thus confirming the negligible spatial dispersion of the fishnet-based PRS. (b) S_{11} (solid lines) and S_{21} (dashed lines) for the TE-TM cross-coupling of a fishnet design with parameters as in Fig. 4(a) at $\phi = 45°$ and $\theta = 0, 40, 80°$ (in blue, red, and green, respectively).

provide very low values of X_s, and thus very high directivities without requiring an extreme, unfeasible variation of its geometrical parameters. Moreover, its remarkably negligible spatial dispersion together with its negligible modal TE-TM coupling allow for a simple but accurate modeling. With these motivations at hand, in the next Section IV we completely characterize the radiating properties of four different FPC-LWAs based on four different fishnet-based PRSs.

IV. FISHNET LAYOUTS

In Fig. 3(c) it is shown that all the pairs g and w which lay on the same iso-line can be employed to design a fishnet-based PRS with a certain impedance value. Hence, we have selected four different pairs of g and w (see Table I for details) to design such impedances. The choice of a specific pair rather than others is mainly due to the easiness of fabrication and the good fulfillment of the homogenization limit, since all the pairs lying on the same iso-reactance line lead to the same antenna performance. The characterization of the surface impedance

Fig. 5: (a) Surface reactance X_s for $\theta = 0°$ vs. frequency f for Layouts 1, 2, 3, and 4 in red, blue, green, and black lines, respectively. (b) 2-D section of the proposed FPC-LWA and its equivalent circuit model. Z_0 and Z_1 are the modal impedances in the air and in the medium, respectively, whereas $k_{x0} = \sqrt{k_0^2 - k_z^2}$ and $k_{x1} = \sqrt{k_0^2 \varepsilon_r - k_z^2}$ are the vertical wavenumbers in the air and in the medium, respectively.

over a frequency range spanning from 0.5 THz to 1.5 THz has been performed to have a frequency-dispersive model of the four fishnets. As shown in Fig. 5(a), almost all designs lead to a reactance with a linear frequency dependence, thus suggesting a dominant inductive behavior. An exception is represented by the last design (see black solid line) which seemingly shows a quadratic behavior. This is easily explained looking at the geometrical parameters of the fishnet used in Layout 4, i.e., $g/p = 0.3$ and $w/p = 0.1$, which reveals a geometry with very narrow strips and a lower filling factor (viz., FF = 0.61) compared to Layout 1 (viz., FF = 0.8). As a consequence, the inductive behavior is less dominant and the impedance is also higher, thus leading to design with lower directivities and higher fractional bandwidths. It is worth noting here that the negligible spatial dispersion of the fishnet allows for safely modeling the impedance $Z_s(f)$ reported in Fig. 5(a) as a function of the frequency f only, without including the dependence on the wavenumber. These models of $Z_s(f)$ have then been implemented in the equivalent circuit model depicted in Fig. 5(b) to perform the dispersion analysis of the structure.

Numerical results are reported in Figs. 6(a)-(d) where the behaviors of the complex-mode normalized phase ($\hat{\beta}_z = \beta_z/k_0$) (solid lines) and attenuation ($\hat{\alpha}_z = \alpha_z/k_0$) constants (dashed lines) are shown in the frequency range 0.5 THz to 1.5 THz for both TE (in green) and TM (in blue) polarizations. From Fig. 6 it is manifest that, as long as the impedance increases (from Fig. 6(a) to Fig. 6(d)), the operating frequency $f_{\rm op}$ (defined as the frequency for which β_z and α_z are equal to each other [26]) increasingly differs from the design frequency $f_0 = 1$ THz (see Table I for a numerical comparison). This would also determine a non-negligible disequalization of the radiating performance over the E- and H-planes as shown in Figs. 6(e)–(l) (see also the last column of Table I for a numerical comparison). Note that the change in the operating frequency can be predicted with good accuracy (as long as $X_s \ll \eta_0$) by means of an
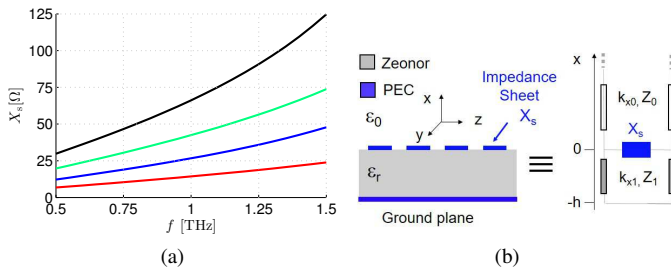
TABLE I: Relevant geometrical parameters and radiating properties of the considered layouts.

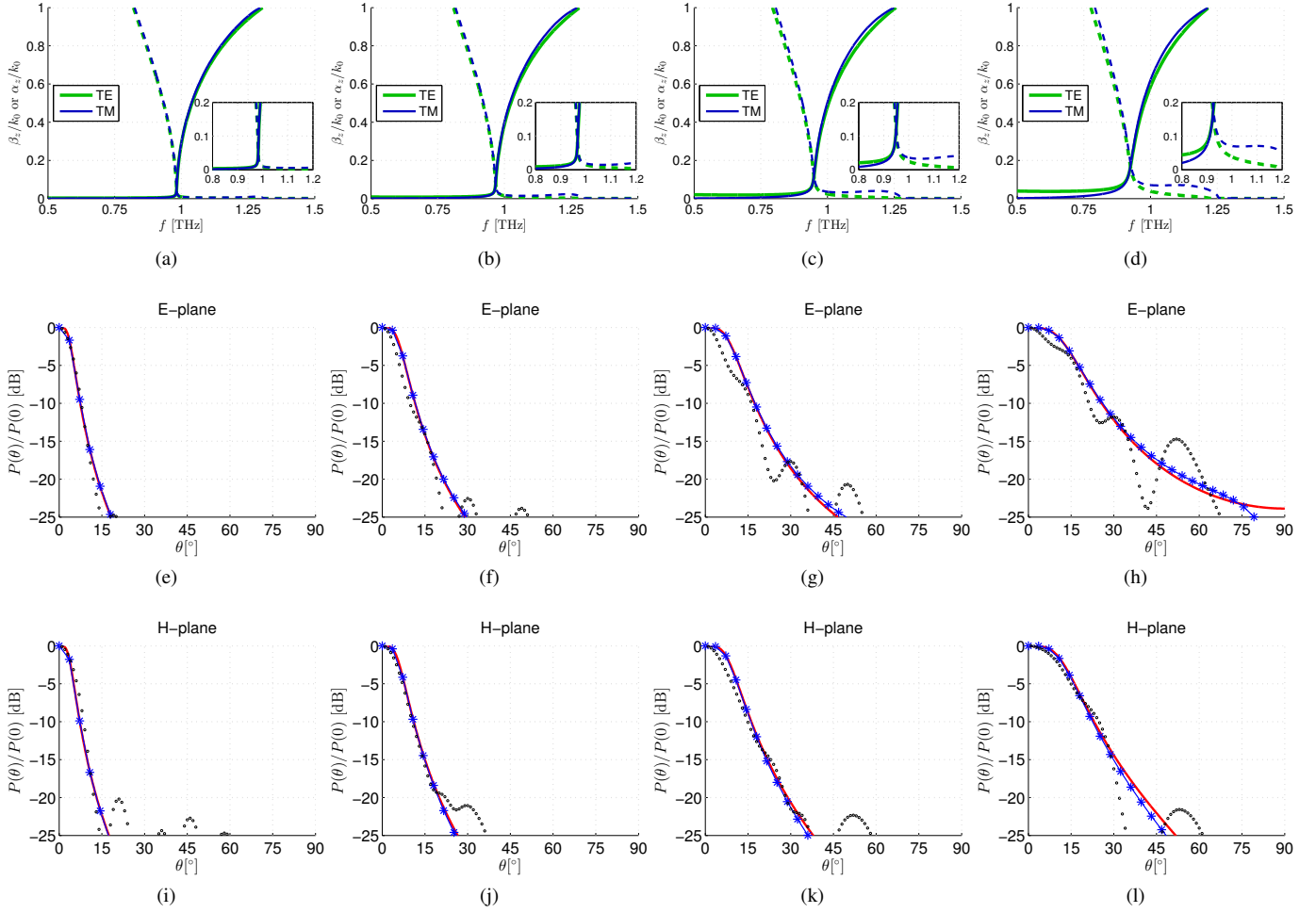| Layout	X_s [Ω]	g/p	w/p	$f_{\rm op}^{\rm TE(TM)}$ [THz]	$BW^{\rm TE(TM)}$ [GHz]	$\hat{\alpha}_z^{\rm TE(TM)}$	$\hat{\alpha}_{\rm loss}$	$e_{r,\infty}$ [%]	e_r [%]	D_0 [dB]	G [dB]	$\Delta\theta^{\rm H(E)}$ [°]
1	15	0.2	0.4	0.982(0.982)	2.34 (2.34)	0.051(0.052)	0.013	75	69	27.74	26.13	8.25(8.42)
2	25	0.2	0.25	0.967(0.967)	5.72 (5.72)	0.079(0.082)	0.008	90	88	23.34	22.96	12.73(13.25)
3	45	0.3	0.2	0.949(0.950)	12.90(12.90)	0.115(0.123)	0.005	96	95	20.23	19.78	18.67(19.98)
4	66	0.3	0.1	0.925(0.926)	29.65(29.68)	0.167(0.186)	0.003	98	98	17.04	16.26	27.09(30.12)

Fig. 6: (a)-(d) Dispersion curves β_z/k_0 (solid lines) and α_z/k_0 (dashed lines) in the spectral range from 0.5 to 1.5 THz for layouts 1 to 4 for TE (in green) and TM (in blue) polarizations. The insets highlight the behavior around $f_{\rm op}$. Radiation patterns normalized to broadside radiation calculated with the leaky-wave approach (red solid lines) and reciprocity theorem (blue asterisks), and validated with full-wave simulations (black circles) are reported over the (e)-(h) E-plane and (i)-(l) H-plane. Results for layouts going from 1 to 4 are shown from (e) to (h) for the E-plane, and from (i) to (l) for the H-plane.

analytical expression [26]:

$$(f_{\rm op} - f_0)/f_0 = \operatorname{arccot}\left[\eta_0/(\sqrt{\varepsilon_r}X_s(f_{\rm op}))\right]/\pi. \qquad (3)$$

Furthermore, a higher reactance X_s increases the normalized attenuation constant at $f_{\rm op}$; this is a predictable effect due to the *weaker* reflectivity of a higher X_s. It is then expected that for higher X_s, the radiation features at broadside will be characterized by wider beamwidths and reduced directivities. This result is confirmed by the radiation patterns obtained through both leaky-wave theory (red solid lines) and reciprocity theorem (blue asterisks) [23], [26], as shown in Figs. 6(e)-(h) for the E-plane (primarily determined by the TM leaky mode)

and in Figs. 6(i)-(l) for the H-plane (primarily determined by the TE leaky mode). The relevant radiating properties of all layouts over both the principal planes are listed in Table I.

It is worth commenting on the expected efficiency of these devices to have a measure of the gain rather than directivity. As a matter of fact, the very low but finite loss tangent of Zeonor [38] contributes to raise the leakage rates in all layouts. Hence, we have determined the amount of leakage due to radiation $\hat{\alpha}_{\rm rad}$ and that due to absorption $\hat{\alpha}_{\rm loss}$ (where $\hat{\alpha}_z = \hat{\alpha}_{\rm loss} + \hat{\alpha}_{\rm rad}$) to calculate the efficiency as proposed in [44]:

$$e_r = e_{r,\infty}\eta_r = (\alpha_{\rm rad}/\alpha_z)\left(1 - e^{-\alpha_z L}\right), \qquad (4)$$

where L is the antenna length along the y- and x-axes, whereas $e_{r,\infty} = \lim_{L\to\infty} e_r$ and η_r are the efficiency contributions due to the substrate losses and due to the finiteness of the structure, respectively. Note that the values of $\alpha_{\rm rad}$ and $\alpha_{\rm loss}$ have been determined by running two different numerical simulations: one of the ideal, lossless structure (to determine $\alpha_{\rm rad}$), and one of the lossy structure (to determine α_z and in turn $\alpha_{\rm loss}$).

The values of $e_{r,\infty}$ and e_r are reported in Table I for $L = 20\lambda_0$ which leads to $\eta_r > 90\%$ for all layouts. As a result, it is possible to calculate the gain as $G = e_r D_0$, which is just fractions of a dB lower than the predicted theoretical directivities, thus confirming the remarkable radiating performance of this kind of devices. Notably, the impact of the substrate loss is more evident for highly-directive layouts leading to an efficiency reduction of more than 20% with respect to the layouts with the lower directivity.

However, both the adopted leaky-wave approach and the reciprocity theorem results assume the structure to be laterally infinite. In addition, numerical results do not take into account a realistic excitation. Hence, we complete the validation of this study by performing full-wave simulations (CST Microwave Studio) for the truncated structures. The structure has then been excited by modeling a y-oriented HMD with a slot of lateral dimensions $\lambda_0/2$ and $\lambda_0/4$ along the y- and x-axis, respectively, for taking care of the technological constraints pointed out in Section II. As expected, [see Figs. 6(e)-(h)] the effect of the lateral truncation ($L = 20\lambda_0$) is almost negligible due to the weak contribution of the field at the edge of the structure ($\eta_r > 90\%$). The agreement between full-wave simulations (small black circles) and both the leaky-wave approach (red solid lines) and reciprocity theorem (blue asterisks) is remarkably good. Some minor differences are observed on the E-plane for the last two layouts [see Figs. 6(g)-(h)] probably due to a weaker validity of the homogenization hypothesis. As a matter of fact, a closer agreement has been observed (not shown here for the sake of brevity) when the period of the unit-cell was set to $p = \lambda_0/10$. However, such a choice would lead to design fishnet-based PRS with mask details at the limit of the standard tolerances for the targeted low-cost large area photolithographic process.

As a final comment, we should note that the same simulations have been performed by assuming a thick lossy layer of Al (thick enough to be larger than its skin depth at 1 THz) in place of the ideal PEC modeling the metallic part of the fishnet-like element. However, there were no appreciable differences in the results, except for a considerably longer computational time, so we decided not to show the results. For the same motivations, we have not shown results considering possible errors due to fabrication process, such as the misalignment of the slot with respect to the center of the structure, and a rotation of the slot with respect to the transverse plane. In particular, we have verified by full-wave simulations that a misalignment (with respect to the center) of the slot of 10 μm in the transverse plane, and a rotation around the vertical axis of about 15 mrad barely affect the symmetry of the radiation pattern below the sidelobe level (around -20 dB). This is a further confirmation of the validity of the homogenization limit. However, we should note that coupling losses may arise due to imperfect mechanical coupling between the feeding waveguide and the slot and due to trapped humidity.

V. CONCLUSION

In this work, we have addressed the design of FPC-LWAs in the THz range proposing a systematic approach for the modeling of homogenized metasurfaces. Taking advantage of an original ad-hoc model for the full-wave characterization of metasurfaces, we have evaluated the electromagnetic response (in terms of homogenized impedance) of various printed PRS to identify a suitable topology for the THz design of a highly-directive FPC-LWAs. As a result, a fishnet-like topology has been identified as a privileged candidate for four different FPC-LWAs which achieve theoretical directivities spanning from 15 dB to 30 dB. After a rigorous theoretical and numerical analysis based on the leaky-wave approach, the radiating properties of the proposed layouts have been evaluated and validated through full-wave simulations, showing a close agreement with the theoretical prediction as well as a very promising radiating performance. The proposed method may result a particularly useful tool for a robust and reliable design of FPC-LWAs in the THz range in view of their experimental realization.

REFERENCES

[1] G. P. Williams, "Filling the THz gap - high power sources and applications," *Rep. Prog. Phys.*, vol. 69, no. 2, p. 301, 2005.

[2] C. Armstrong, "The truth about terahertz," *IEEE Spectrum*, vol. 9, no. 49, pp. 36–41, Sep. 2012.

[3] V. Petrov, A. Pyattaev, D. Moltchanov, and Y. Koucheryavy, "Terahertz band communications: Applications, research challenges, and standardization activities," in *8th Int. Congress Ultra Modern Telecom. Control Systems and Workshops (ICUMT)*, 18-20 Oct. 2016, Lisbon, Portugal, pp. 183–190.

[4] V. M. Lubecke, K. Mizuno, and G. M. Rebeiz, "Micromachining for terahertz applications," *IEEE Trans. Microw. Theory Techn.*, vol. 46, no. 11, pp. 1821–1831, 1998.

[5] G. M. Rebeiz, "Millimeter-wave and terahertz integrated circuit antennas," *Proceedings of the IEEE*, vol. 80, no. 11, pp. 1748–1770, 1992.

[6] G. Chattopadhyay, T. Reck, C. Lee, and C. Jung-Kubiak, "Micromachined packaging for terahertz systems," *Proc. IEEE*, vol. 105, no. 6, Jun. 2017.

[7] P. U. Jepsen and S. Keiding, "Radiation patterns from lens-coupled terahertz antennas," *Opt. Lett.*, vol. 20, no. 8, pp. 807–809, 1995.

[8] J. Van Rudd, J. L. Johnson, and D. M. Mittleman, "Cross-polarized angular emission patterns from lens-coupled terahertz antennas," *JOSA B*, vol. 18, no. 10, pp. 1524–1533, 2001.

[9] N. Llombart, C. Lee, M. Alonso-del Pino, G. Chattopadhyay, C. Jung-Kubiak, L. Jofre, and I. Mehdi, "Silicon micromachined lens antenna for Thz integrated heterodyne arrays," *IEEE Trans. THz Sci. Tech.*, vol. 3, no. 5, pp. 515–523, Sep. 2013.

[10] G. V. Eleftheriades, W. Y. Ali-Ahmad, L. P. Katehi, and G. M. Rebeiz, "Millimeter-wave integrated-horn antennas. I. Theory," *IEEE Trans. Antennas Propag.*, vol. 39, no. 11, pp. 1575–1581, 1991.

[11] W. Y. Ali-Ahmad, G. V. Eleftheriades, L. P. Katehi, and G. M. Rebeiz, "Millimeter-wave integrated-horn antenna. II. Experiment," *IEEE Trans. Antennas Propag.*, vol. 39, no. 11, pp. 1582–1586, 1991.

[12] G. V. Eleftheriades and G. M. Rebeiz, "Design and analysis of quasi-integrated horn antennas for millimeter and submillimeter-wave applications," *IEEE Trans. Microw. Theory Tech.*, vol. 41, no. 6, pp. 954–965, 1993.

[13] M. Jablan, H. Buljan, and M. Soljačić, "Plasmonics in graphene at infrared frequencies," *Phys. Rev. B*, vol. 80, no. 24, p. 245435, 2009.

[14] M. Tamagnone, J. S. Gómez-Díaz, J. R. Mosig, and J. Perruisseau-Carrier, "Analysis and design of terahertz antennas based on plasmonic resonant graphene sheets," *J. App. Phys.*, vol. 112, no. 11, p. 114915, 2012.

[15] J. M. Jornet and I. F. Akyildiz, "Graphene-based nano-antennas for electromagnetic nanocommunications in the terahertz band," in *4th Eur. Conf. Antennas Propag. (EuCAP)*, 12-16 April 2010, Barcelona, Spain, pp. 1–5.

[16] M. Esquius-Morote, J. S. Gómez-Díaz, and J. Perruisseau-Carrier, "Sinusoidally modulated graphene leaky-wave antenna for electronic beamscanning at THz," *IEEE Trans. THz Sc. Tech.*, vol. 4, no. 1, pp. 116–122, 2014.

[17] W. Fuscaldo, P. Burghignoli, P. Baccarelli, and A. Galli, "Graphene Fabry-Perot cavity leaky-wave antennas: Plasmonic versus nonplasmonic solutions," *IEEE Trans. Antennas Propag.*, vol. 65, no. 4, pp. 1651–1660, Apr. 2017.

[18] ——, "Complex mode spectra of graphene-based planar structures for THz applications," *J. Infrared Milli. Terahz Waves*, vol. 36, no. 8, pp. 720–733, Aug. 2015.

[19] ——, "A reconfigurable substrate-superstrate graphene-based leaky-wave THz antenna," *IEEE Antennas Wireless Propag. Lett.*, vol. 15, pp. 1545–1548, 2016.

[20] W. Zouaghi, D. Voß, M. Gorath, N. Nicoloso, and H. G. Roskos, "How good would the conductivity of graphene have to be to make single-layer-graphene metamaterials for terahertz frequencies feasible?" *Carbon*, vol. 94, pp. 301–308, 2015.

[21] M. Tamagnone and J. R. Mosig, "Theoretical limits on the efficiency of reconfigurable and nonreciprocal graphene antennas," *IEEE Antennas Wireless Propag. Lett.*, vol. 15, pp. 1549–1552, 2016.

[22] M. Tamagnone, A. Fallahi, J. R. Mosig, and J. Perruisseau-Carrier, "Fundamental limits and near-optimal design of graphene modulators and non-reciprocal devices," *Nat. Photonics*, vol. 8, no. 7, pp. 556–563, 2014.

[23] D. R. Jackson and A. A. Oliner, "Leaky-Wave Antennas," in *Modern Antenna Handbook*, C. A. Balanis, Ed.   New York, NY, USA: John Wiley & Sons, 2011, ch. 7.

[24] S. Tretyakov, *Analytical Modeling in Applied Electromagnetics*.   Norwood, MA, USA: Artech House, 2003.

[25] C. L. Holloway, E. F. Kuester, J. A. Gordon, J. O'Hara, J. Booth, and D. R. Smith, "An overview of the theory and applications of metasurfaces: The two-dimensional equivalents of metamaterials," *IEEE Antennas Propag. Mag.*, vol. 54, no. 2, pp. 10–35, Apr. 2012.

[26] G. Lovat, P. Burghignoli, and D. R. Jackson, "Fundamental properties and optimization of broadside radiation from uniform leaky-wave antennas," *IEEE Trans. Antennas Propag.*, vol. 54, no. 5, pp. 1442–1452, May 2006.

[27] T. Zhao, D. R. Jackson, J. T. Williams, and A. A. Oliner, "General formulas for 2-D leaky-wave antennas," *IEEE Trans. Antennas Propag.*, vol. 53, no. 11, pp. 3525–3533, 2005.

[28] O. Luukkonen, C. Simovski, G. Granet, G. Goussetis, D. Lioubtchenko, A. V. Raisanen, and S. A. Tretyakov, "Simple and accurate analytical model of planar grids and high-impedance surfaces comprising metal strips or patches," *IEEE Trans. Antennas Propag.*, vol. 56, no. 6, pp. 1624–1632, Jun. 2008.

[29] W. Fuscaldo, S. Tofani, D. C. Zografopoulos, P. Baccarelli, P. Burghignoli, R. Beccherelli, and A. Galli, "Tunable Fabry-Perot cavity THz antenna based on leaky-wave propagation in nematic liquid crystals," *IEEE Antennas Wireless Propag. Lett.*, vol. 16, pp. 2046–2049, 2017.

[30] D. C. Zografopoulos and R. Beccherelli, "Tunable terahertz fishnet metamaterials based on thin nematic liquid crystal layers for fast switching," *Scientific Rep.*, vol. 5, no. 13137, 2015.

[31] B. Vasić, D. C. Zografopoulos, G. Isić, R. Beccherelli, and R. Gajić, "Electrically tunable terahertz polarization converter based on overcoupled metal-isolator-metal metamaterials infiltrated with liquid crystals," *Nanotechnology*, vol. 28, no. 12, p. 124002, 2017.

[32] D. R. Jackson and A. A. Oliner, "A leaky-wave analysis of the high-gain printed antenna configuration," *IEEE Trans. Antennas Propag.*, vol. 36, no. 7, pp. 905–910, Jul. 1988.

[33] D. R. Jackson, A. A. Oliner, and A. Ip, "Leaky-wave propagation and radiation for a narrow-beam multiple-layer dielectric structure," *IEEE Trans. Antennas Propag.*, vol. 41, no. 3, pp. 344–348, Mar. 1993.

[34] A. B. Yakovlev, O. Luukkonen, C. R. Simovski, S. A. Tretyakov, S. Paulotto, P. Baccarelli, and G. W. Hanson, "Analytical modeling of surface waves on high impedance surfaces," in *Metamaterials and Plasmonics: Fundamentals, Modelling, Applications*.   Dordrecht, The Netherlands: Springer, 2009, pp. 239–254.

[35] T. Tamir and A. A. Oliner, "Guided complex waves. Part 1: fields at an interface," *Proc. IEE*, vol. 110, no. 2, pp. 310–324, Feb. 1963.

[36] ——, "Guided complex waves. Part 2: relation to radiation patterns," *Proc. IEE*, vol. 110, no. 2, pp. 325–334, Feb. 1963.

[37] A. Ip and D. R. Jackson, "Radiation from cylindrical leaky waves," *IEEE Trans. Antennas Propag.*, vol. 38, no. 4, pp. 482–488, Apr. 1990.

[38] P. A. George, W. Hui, F. Rana, B. G. Hawkins, A. E. Smith, and B. J. Kirby, "Microfluidic devices for terahertz spectroscopy of biomolecules," *Opt. Express*, vol. 16, no. 3, pp. 1577–1582, 2008.

[39] "VDI Virginia Diodes, Inc., Waveguide band designations." [Online]. Available: http://vadiodes.com/VDI/pdf/waveguidechart200908.pdf

[40] Y. H. Lo and R. Leonhardt, "Aspheric lenses for terahertz imaging," *Opt. Express*, vol. 16, no. 20, pp. 15 991–15 998, 2008.

[41] A. Ferraro, D. C. Zografopoulos, R. Caputo, and R. Beccherelli, "Broad-and narrow-line terahertz filtering in frequency-selective surfaces patterned on thin low-loss polymer substrates," *IEEE J. Sel. Topics Quantum Electron.*, vol. 23, no. 4, pp. 1–8, 2017.

[42] W. Fuscaldo, G. Valerio, A. Galli, R. Sauleau, A. Grbic, and M. Ettorre, "Higher-order leaky-mode Bessel-beam launcher," *IEEE Trans. Antennas Propag.*, vol. 64, no. 3, pp. 904–913, Mar. 2016.

[43] A. Epstein, J. P. Wong, and G. V. Eleftheriades, "Cavity-excited Huygens' metasurface antennas for near-unity aperture illumination efficiency from arbitrarily large apertures," *Nat. Commun.*, vol. 7, p. 10360, 2016.

[44] C. Di Nallo, F. Frezza, A. Galli, and P. Lampariello, "Rigorous evaluation of ohmic-loss effects for accurate design of traveling-wave antennas," *J. Electromagn. Waves Appl.*, vol. 12, no. 1, pp. 39–58, 1998.

Walter Fuscaldo (S'15) was born in Rome, Italy, in 1987. He received the B.Sc. and M.Sc. (cum laude) degrees in telecommunications engineering from "La Sapienza" University of Rome, Rome, in 2010 and 2013, respectively. In 2017, he received the Ph.D. degree (cum laude and with the *Doctor Europaeus* label) from both the Department of Information Engineering, Electronics and Telecommunications (DIET) and the Institut d'Électronique et de Télécommunications de Rennes (IETR), Université de Rennes 1, Rennes, France, under a cotutelle agreement between the institutions. From September 2014 to December 2014, and from September 2017 to December 2017 he was a Visiting Researcher with the NATO-STO Center for Maritime Research and Experimentation, La Spezia, Italy. From May 2016 to September 2016, he was a Visiting Researcher with the University of Houston, Houston, TX, USA. His current research interests include propagation of leaky waves, surface waves and surface plasmon polaritons, analysis and design of leaky-wave antennas, generation of limited-diffraction limited-dispersion electromagnetic waves, millimeter-wave focusing systems, graphene electromagnetics, metasurfaces, and THz antennas. Dr. Fuscaldo was a recipient of the Yarman-Carlin Student Award at the IEEE 15th Mediterranean Microwave Symposium in 2015, and the Young Engineer Prize for the Best Paper presented at the 46th European Microwave Conference in 2016.

Silvia Tofani (S'16) was born in Rome, Italy, in 1989. She received the B.Sc. degree in clinical engineering and the M.Sc. (cum laude) degree in nanotechnology engineering from "La Sapienza" University of Rome, in 2011 and 2014, respectively. From March 2014 to May 2014, she was a Visiting Student at Warsaw Military University, Warsaw, Poland. From June 2014 to October 2014, she was a Research Fellow at Institute for Microelectronics and Microsystems, National Research Council of Italy, Rome. In November 2014, she started a PhD in Applied Electromagnetics at "La Sapienza" University of Rome in collaboration with Institute for Microelectronics and Microsystems, National Research Council of Italy, Rome. In February 2016 she was a Visiting Student at Insitut National de la Recherche Scientifique, Varennes (Qubec), Canada. Her research interests include terahertz diffractive optics, devices characterization at terahertz frequencies, analysis and design of leaky-wave antennas, numerical studies of liquid crystal devices, and interactions between electromagnetic fields and macromolecular structures for drug delivery.

Dimitrios C. Zografopoulos was born in Thessaloniki, Greece, in 1980. He received the Diploma in Electrical and Computer Engineering and the Doctorate degree from the Aristotle University of Thessaloniki (AUTH), Thessaloniki, Greece, in 2003 and 2009, respectively. In 2010, he was a Postdoctoral Fellow of the Research Committee of the AUTH and in 2011 a Post-doctoral Research Fellow of the Greek States Scholarship Foundation and a Visiting Research Fellow at the Department of Electronics Technology, Carlos III University of Madrid. He subsequently moved under a two-year Intra-European Marie-Curie Fellowship to the Institute for Microelectronics and Microsystems of the Italian National Research Council of Italy, Rome, where he is currently employed as a Researcher. His research interests include the design and analysis of photonic/plasmonic waveguides, tunable metamaterials and components for electromagnetic wave manipulation, as well as the study of liquid-crystal physics. He is the author or coauthor of more than 50 scientific papers in international journals and 2 book chapters.
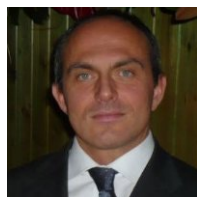

Paolo Burghignoli (S'97-M'01-SM'08) was born in Rome, Italy, on February 18, 1973. He received the Laurea degree (*cum laude*) in electronic engineering and the Ph.D. degree in applied electromagnetics from "La Sapienza" University of Rome, Rome, Italy, in 1997 and 2001, respectively. In 1997, he joined the Electronic Engineering Department, now Department of Information Engineering, Electronics and Telecommunications, "La Sapienza" University of Rome. From January 2004 to July 2004, he was a Visiting Research Assistant Professor with the University of Houston, Houston, TX. From November 2010 to October 2015, he was an Assistant Professor with "La Sapienza" University of Rome and since November 2015 he has been an Associate Professor with the same University. In March 2017 he received the National Scientific Qualification for the role of Full Professor of Electromagnetic Fields in Italian Universities. His scientific interests include analysis and design of planar antennas and arrays, leakage phenomena in uniform and periodic structures, numerical methods for integral equations and periodic structures, propagation and radiation in metamaterials, electromagnetic shielding, and graphene electromagnetics. Dr. Burghignoli was the recipient of the "Giorgio Barzilai" Laurea Prize (1996–1997) presented by the former IEEE Central & South Italy Section, a 2003 IEEE MTT-S Graduate Fellowship, and a 2005 Raj Mittra Travel Grant for Junior Researchers presented at the IEEE AP-S Symposium on Antennas and Propagation, Washington, DC. He is a coauthor of the "Fast Breaking Papers, October 2007" in EE and CS, about metamaterials (paper that had the highest percentage increase in citations in Essential Science Indicators, ESI).

Paolo Baccarelli (M'01) received the Laurea degree in electronic engineering and the Ph.D. degree in applied electromagnetics from "La Sapienza" University of Rome, Rome, Italy, in 1996 and 2000, respectively. In 1996 he joined the Department of Electronic Engineering, "La Sapienza" University of Rome, where he was an Assistant Professor since November 2010. From April 1999 to October 1999, he was a Visiting Researcher with the University of Houston, Houston, TX. In 2017, he joined the Department of Engineering, University of "Roma Tre", Rome, Italy, where he has been an Associate Professor since July 2017. In December 2017, he received the National Scientific Qualification for the role of Full Professor of Electromagnetic Fields in Italian Universities. He has co-authored about 230 papers in international journals, conference proceedings, and book chapters. His research interests include analysis and design of planar antennas and arrays, leakage phenomena in uniform and periodic structures, numerical methods for integral equations and periodic structures, propagation and radiation in anisotropic media, metamaterials, graphene, and electromagnetic band-gap structures. Dr. Baccarelli was the recipient of the "Giorgio Barzilai" Laurea Prize (1994-1995) presented by the former IEEE Central & South Italy Section; he is in the editorial board of international journals and acts as reviewer for more than 20 IEEE, IET, OSA, and AGU journals; he was a Secretary of the "2009-European Microwave Week" (EuMW 2009) and has been member of the TPCs of several international conferences.

Romeo Beccherelli was born in Plovdiv, Bulgaria, in 1969. He received the Laurea degree cum laude and the Ph.D. degree both in electronic engineering from "La Sapienza" University of Rome, Italy, in 1994 and 1998, respectively. In 1997 and 2001, he was a Visiting Researcher Fellow at the Department of Physics-Division of Microelectronics and Nanoscience-Chalmers University of Technology, Gothemburg, Sweden. He served in the technical Corps of the Italian Army as a Second Lieutenant. In 1997, he joined the Department of Engineering Science, University of Oxford, Oxford, U.K. as a Postdoctoral Research Assistant and in 2000 the Department of Electronic Engineering, "La Sapienza" University of Rome, Italy, as a Research Fellow. In 2001, he was appointed Researcher and in 2006 a Senior Researcher at the Institute for Microelectronics and Microsystems, National Research Council of Italy, Rome. He is an inventor of two patents and author of approximately 70 scienfic papers in international journals, 80 conference proceedings papers and three book chapters. He has been a Principal Investigator in research projects funded by the European Community, the European Space Agency and by the Italian Government, and co-coordinator of four bilateral projects. His initial research interests in liquid crystal display technology have evolved into sensor arrays, photonics and plasmonics based on liquid crystals, and into metamaterial and metasurface devices and systems for processing microwaves and terahertz waves. His doctoral thesis was awarded the International Otto Lehman Prize 1999 in liquid crystal technology by the University of Karlsruhe, Germany and the Otto Lehmann Foundation.

Alessandro Galli (S'91-M'96) received the Laurea degree in Electronic Engineering and the Ph.D. degree in Applied Electromagnetics from "La Sapienza" University of Rome, Italy, in 1990 and 1994, respectively. Since 1990, he has been with the Department of Electronic Engineering (now Department of Information Engineering, Electronics, and Telecommunications) of "La Sapienza" University of Rome. In 2000 he became an Assistant Professor, and in 2002 an Associate Professor at "La Sapienza" University of Rome; in 2013 he passed the National Scientific Qualification as a Full Professor in the sector of Electromagnetics. For the educational activities, he is currently teaching the courses of "Electromagnetic Fields," "Advanced Antenna Engineering," and "Engineering Electromagnetics" for Electronics and Communications Engineering at Sapienza University of Rome. He has authored more than 300 papers on journals, books, and conferences. His research interests include theoretical and applied electromagnetics, mainly focused on modeling, numerical analysis, and design for antennas and passive devices from microwaves to terahertz: specific topics involve leaky waves, periodic and multilayered printed structures, metamaterials, and graphene. Other topics of interest involve geoelectromagnetics, bioelectromagnetics, and microwave plasma heating for alternative energy sources. He is author of a patent for an invention concerning a type of microwave antenna. Dr. Galli was elected as the Italian representative of the Board of Directors of the "European Microwave Association" (EuMA), the main European Society of electromagnetics, for the 2010-2012 triennium and then re-elected for the 2013-2015 triennium. He was the General Co-chair of the "European Microwave Week" (EuMW), the most important conference event in the electromagnetic area at European level in 2014. Since its foundation in 2012, he is the Coordinator of the "European Courses on Microwaves" (EuCoM), the first European educational institution on microwaves. He is also a member of the "European School of Antennas" (ESoA). He is a member of the leading scientific societies of electromagnetics, and an Associate Editor of the "International Journal of Microwave and Wireless Technologies" (Cambridge University Press) and of the "IET Microwaves, Antennas & Propagation" (Institution of Engineering and Technology). He was the recipient of various grants and prizes for his research activity: he won in 1994 the "Barzilai Prize" for the best scientific work of under-35 researchers at the "10th National Meeting of Electromagnetics", and in 1994 and 1995 the "Quality Presentation Recognition Award" at the International Microwave Symposium by the "Microwave Theory and Techniques" (MTT) Society of the Institute of Electrical and Electronics Engineering (IEEE).